Published in final edited form as:
Skeletal Radiol. 2012 February ; 41(2): 209–217. doi:10.1007/s00256-011-1331-z.

A synthetic cartilage extracellular matrix model: hyaluronan and collagen hydrogel relaxivity, impact of macromolecular concentration on dGEMRIC

Ediuska Laurens,
Department of Biomedical Engineering, The Cleveland Clinic, Cleveland, OH, USA, Stryker Craniomaxillofacial, Stryker Corporation, Mahwah, NJ, USA

Erika Schneider,
Imaging Institute, The Cleveland Clinic, 9500 Euclid Avenue, HB6, Cleveland, OH 44195, USA

Carl S. Winalski, and
Department of Biomedical Engineering, The Cleveland Clinic, Cleveland, OH, USA, Imaging Institute, The Cleveland Clinic, 9500 Euclid Avenue, HB6, Cleveland, OH 44195, USA

Anthony Calabro
Department of Biomedical Engineering, The Cleveland Clinic, Cleveland, OH, USA

Ediuska Laurens: ediuska.laurens@stryker.com; Erika Schneider: schneie1@ccf.org; Carl S. Winalski: winalsc@ccf.org; Anthony Calabro: calabra@ccf.org

Abstract

Objective—To develop and characterize the MR properties of a synthetic model for cartilage extracellular matrix using hydrogels and to determine the concentration dependence of spin–lattice (T1) and spin-spin (T2) relaxation times of hydrogels and their glycosaminoglycan and collagen components in the presence and absence of gadopentetate dimeglumine (Gd-DTPA) for use in dGEMRIC.

Materials and methods—T1 and T2 measurements were made at 3 Tesla on a range of gelatin (i.e., collagen) and hyaluronan (i.e., glycosaminoglycan) solutions (6.25–100 g/l), alone, together in a composite, and as dityramine-bridged hydrogels. Relaxivity was calculated as a function of macro-molecular concentration.

Results—Even at the highest concentrations, gelatin and hyaluronan solutions had T1 and T2 values significantly larger than those reported for cartilage. Only composite hydrogels with gelatin and hyaluronan concentrations naturally found in cartilage resulted in T1 values, but not T2 values, representative of cartilage. Relaxivities were slightly dependent on both hyaluronan concentration (R1= 0.0027 l g^{-1} s^{-1}; R2=0.025 l g^{-1} s^{-1}) and gelatin concentration (R1=0.0032 l g^{-1} s^{-1}; R2=0.020 l g^{-1} s^{-1}) alone and as a composite (R1=0.0068 l g^{-1} s^{-1}; R2=0.101 l g^{-1} s^{-1}). Gd-DTPA relaxivities were dependent upon macromolecular concentration and varied by 14–32% (R1=4.24 to 5.55 mM^{-1} s^{-1}; R2=4.60 to 6.27 mM^{-1} s^{-1}) over the range of cartilage biochemistry.

Conclusions—Without the contrast agent, hyaluronan and gelatin, alone or in a composite, have a very small impact on the relaxivities of the model system. The impact on R1 was approximately tenfold less than on R2. In contrast, macromolecular concentrations above 50 g/l significantly

Correspondence to: Erika Schneider, schneie1@ccf.org.

Conflict of interest AC is an inventor of the hydrogel technology, which is licensed to Lifecore Biomedical, Inc.

impacted Gd-DTPA relaxivity and should be accounted for when measuring the glycosaminoglycan content of cartilage in vivo using dGEMRIC.

Introduction

Current research in osteoarthritis often involves magnetic resonance (MR) evaluation of cartilage biochemistry including the proteoglycan, i.e., glycosaminoglycan (GAG), and collagen concentration of articular and meniscal cartilage [1–30]. While many MR acquisitions are sensitive to matrix composition, some approaches have greater specificity for one molecular species compared to others, although their sensitivities to collagen and GAG content may be interdependent [1–5, 14, 31]. For example, decreased collagen content, fibrillation, and clefts have been correlated with cartilage lesions found on T2-weighted images and T2 relaxation time maps [1–4, 14]. In addition, T1 relaxation time maps obtained using delayed-gadolinium enhanced MR imaging of cartilage (dGEMRIC) are used to display and compute local GAG concentration within cartilage [1–4, 6, 8, 10–30, 32].

Glycosaminoglycans and collagen are major components of most tissue extracellular matrices including articular and meniscal cartilage. In this study, tyramine-based hydrogels are used as synthetic model for extracellular matrices. Tyramine-based hyaluronan (TB-HA) hydrogels [33–42], currently under development for tissue engineering applications, and a collagen hydrogel (TB-GE) [43–45], based on commercial gelatin in various concentrations, are used to explore the relationship between hyaluronan, gelatin, and composite concentrations on T1 and T2 relaxation times. Dityramine cross-linking provides structure to hyaluronan monomers and stabilizes it to dissolution, similar to the intrinsic gelation of monomers in gelatin and agar. The effect of the cross-linking during hydrogel formation is also evaluated. The concentration dependence found from these relaxation time measurements may enable quantification of TB-hydrogels within in vivo tissue engineering and repair applications.

Most dGEMRIC studies calculate GAG content by assuming Gd-DTPA relaxivity is independent of tissue macromolecular concentration even though contradictory evidence exists. One study [6] found the Gd-DTPA relaxivity in cartilage was consistent across a range of GAG concentrations. Another [8] concluded that macromolecular concentration, but not molecule type, can increase the relaxivity of Gd-DPTA in cartilage by 30–70% compared to that in saline. In ex vivo cartilage plugs with varying levels of trypsin digestion, a third manuscript [9] reported the relaxivity of Gd-DPTA was influenced by the level of GAG depletion. The specifics of the relaxivity dependence may be important given the increasing use of dGEMRIC techniques in clinical research. However, it is difficult to manipulate the individual components of cartilage in a controlled and uniform manner. In an attempt to resolve this issue, we investigated the influence of the individual components of cartilage extracellular matrix (TB-HA, TB-GE) and composite cartilage extracellular matrix (TB-CO) on the relaxivity of Gd-DTPA, as it would be applied in dGEMRIC.

Materials and methods

Synthesis

The compositions and concentrations of the materials studied are described in Table 1. Corgel™ Biohydrogel (hyaluronan with a 5% degree of tyramine substitution; TS-HA) was manufactured by Lifecore Biomedical, Inc., Chaska, MN, using a process adapted from Darr et al. [33]. Hyaluronan, sodium salt (MW > 1 million Daltons) was also obtained from Lifecore Biomedical. Gelatin (300 bloom), agar, tyramine hydrochloride, *N*-hydroxysuccinimide, 1-ethyl-3-(3-dimethylaminopropyl) carbodiimide, sodium chloride, type II horseradish peroxidase, and hydrogen peroxide were obtained from Sigma, St. Louis,

MO. Sodium hydroxide and 2-(*N*-morpholino)ethanesulfonic acid were purchased from Fisher Chemicals, Pittsburgh, PA. Phosphate buffered saline (PBS) solutions (1× and 10×) were purchased in house. Magnevist (Gd-DTPA) was obtained from Bayer Healthcare Pharmaceuticals, Park Ridge, NJ.

The synthesis of both the tyramine-based hyaluronan (TB-HA) [33, 42] and gelatin hydrogels (TB-GE) [43–45] has been previously published; we present the minimum changes in this chemistry necessary to reproduce the ECM results. TB-GE is synthesized [45–47] using the same chemistry as TB-HA hydrogels [33, 42] and has the same amino acid composition as type-1 collagen with a broad distribution of molecular weights [46]. The degree of tyramine substitution on TS-GE was determined by amino acid analysis of TS-GE samples using cation exchange chromatography based on Spackman et al. [47] through the Molecular Biology-Proteomics Facility, University of Oklahoma.

TB-HA hydrogels were first cross-linked in ultrapure water then equilibrated in PBS. The TB-HA hydrogels at 6.25, 12.5, and 25 g/l were found to shrink ~30–35% by volume; while the hydrogels at 50 and 100 g/l swelled no more than 10% by volume. For the TB-HA and TB-CO hydrogels, the observed shrinkage or swelling in PBS was sufficiently reproducible that the linear correlation curves (not shown) of initial (in water) versus final (in PBS) concentration could be used to form hydrogels with concentrations equivalent to unsubstituted and tyramine-substituted samples. The TB-GE hydrogels were found to shrink in PBS to a final concentration range below that necessary to prepare these hydrogels at 6.25, 12.5, 25, 50, and 100 g/l; therefore, these samples were prepared in ultrapure water.

To cross-link the gels, the lyophilized materials were resuspended in appropriate volumes of ultrapure water containing 10 U/ml of horseradish peroxidase, allowed to fully hydrate, and cross-linked upon addition of dilute hydrogen peroxide. After the hydrogels fully cured overnight at 4°C, an appropriate volume of 10× PBS was added to each sample to give a final 1× concentration of PBS, and the samples allowed to equilibrate (shrink or swell) in PBS overnight at 4°C. After equilibration, the samples were viewed under UVB light (280–320 nm) to confirm complete and uniform cross-linking based on the uniformity and intensity of their fluorescence relative to standards. A hexuronic acid assay was used to quantify hyaluronan concentration [48].

Agar (0.5–4 wt%) and Gd-DTPA (0.125–2 mM) were prepared in 1 ml of PBS and were used as controls. Additional controls were provided by 1 ml aliquots of ultrapure water and PBS.

Relaxation time measurements

The relaxation time measurements were performed on 1.5 ml samples at room temperature and 3 Tesla (Tim TRIO; Siemens Medical Solutions, Erlangen, Germany) using a quadrature transmit/receive head coil. Spin–lattice (T1) relaxation time measurements used an inversion recovery turbo spin echo (TSE) sequence with repetition time (TR) 6,000 ms, echo time (TE) 10 ms and inversion recovery times (TI) of 23, 75, 150, 300, 750, 1,400, 2,000, and 2,800 ms. Spin-spin (T2) relaxation times were measured using a spin echo Carr-Purcell-Meiboom-Gill (CPMG) sequence with TR 6,000 ms and 32 echoes [49] with an echo spacing of 15 ms spanning the range of 15–480 ms. Both T1 and T2 measurements were obtained using a single coronal slice with a field-of-view 260 mm×130 mm, slice thickness 1.9 mm, matrix 256×128 and 1 average.

Relaxation time maps were computed using MRIMapper (MIT, Cambridge, MA) and MATLAB (MathWorks, Natick, MA). Regions of interest (ROIs) were selected as 4×4 to 6×6 pixels from the center of each sample. T1 maps were calculated using a three-parameter

exponential fit $M_{xy} = M_0 * [1 - 2 * (1 - \cos\theta) * \exp -TI/T1) + \exp(-TR/T1)]$, where M_{xy} is the pixel signal intensity obtained at TI, M_o is the signal intensity that would be obtained from the sample in the fully relaxed state, and θ is the flip angle of the inversion pulse. T2 maps were calculated using $M_{xy} = M_o*\exp(-TE/T2)$, where M_{xy} is the pixel signal intensity obtained at TE and M_o is as above. For T2 calculations, the first TE point was excluded from the curve fit [13]. The reported T1 or T2 value was the average from the ROI of each sample.

The mean T1 and T2 values were utilized to calculate material relaxivity R1 and R2, respectively, using a least-squares fit to the slope of $[1/T1 - 1/T1_{pbs}]$ or $[1/T2 - 1/T2_{pbs}]$ versus macromolecule concentration. For the uncross-linked hyaluronan, gelatin, and composite materials suspended in various Gd-DTPA solutions, the R1 and R2 values were calculated as the slope of $[1/T1_{material\ without\ Gd} - 1/T1_{material\ with\ Gd}]$ or $[1/T2_{material\ without\ Gd} - 1/T2_{material\ with\ Gd}]$ versus Gd-DTPA concentration for each macromolecule and concentration separately.

Statistical analysis

One-way analysis of variance (ANOVA) and Student-Newman-Keuls statistical analyses were used to detect statistically significant changes when comparing relaxivities with a confidence level of 95% ($p<0.05$). The relaxivities of hyaluronan, gelatin, and composite materials in solution were compared to those of the tyramine-substituted and cross-linked formulations of these biomaterials. The relaxivity of Gd-DTPA in hyaluronan, gelatin, and composite materials at various concentrations (6.25, 12.5, 25, 50, and 100 g/l) were compared to Gd-DTPA in PBS as control.

Results

Relaxation times and relaxivities

The T1 and T2 values for each material are presented in Table 2. Figure 1 provides examples of plots of the mean T1 and T2 values for each material measured in an individual imaging session versus material concentration, as the relationship of $[1/T1 - 1/T1_{pbs}]$ and $[1/T2 - 1/T2_{pbs}]$ versus concentration. The average relaxivity for all imaging sessions for each material are summarized in Table 3.

The PBS and water control samples had long T1 and T2 values and varied <5% across all imaging sessions. The T1 and T2 relaxation times decreased linearly with increasing concentration of Gd-DTPA (R1=5.32±0.32 $mM^{-1}\ s^{-1}$, R2=6.05±0.42 $mM^{-1}\ s^{-1}$) and were consistent with values reported in the literature [5, 6]. Increasing agar concentration showed no effect on T1 values (R1=0.028±0.011 $wt\%^{-1}\ s^{-1}$), but a large effect on T2 values (R2=5.91±0.55 $wt\%^{-1}\ s^{-1}$). Direct comparison of agar relaxation times with the literature could not be made as prior work used different concentrations and conditions. The R2 for agar is large and is closer to that of Gd-DTPA than either hyaluronan or gelatin (Table 3).

Both the hyaluronan and gelatin T1 and T2 values decreased slightly, relaxivities were 2–3 orders of magnitude less than Gd-DTPA with increasing concentration, but the effect was independent of tyramine substitution or cross-linking (Table 2). The composite samples (CO, TS-CO, TB-CO), with 1:1 concentrations of hyaluronan and gelatin, showed appreciably larger relaxivities than for either the hyaluronan or gelatin alone. The 50 g/l and 100 g/l composite samples, which had HA and collagen concentrations similar to native cartilage, demonstrated T1 values characteristic of cartilage (700–1250 ms) [5, 32, 50].

Despite the very small R1 and R2 values of hyaluronan, gelatin, and the composite materials, a selective effect of tyramine-substitution and cross-linking was observed (Table

3). Tyramine-substitution had little effect on R1 or R2 values for hyaluronan. However cross-linking increased the R2 value for hyaluronan without affecting R1. Both R1 and R2 for gelatin noticeably decreased upon tyramine substitution. Upon cross-linking, R1 increased for gelatin, but R2 did not change compared to TS-GE. Finally, R1 for the composite samples increased with tyramine substitution, but R2 did not change. Cross-linking lowered both R1 and R2 of the composite samples. The only samples having statistically different relaxivities were the R2 values for hyaluronan (p=0.007) and TS-HA (p=0.012) versus the cross-linked TB-HA, and the R2 values of the composite (p=0.020) and TS-CO (p= 0.019) versus the cross-linked TB-CO.

Gd-DTPA relaxivity

The relaxivities of Gd-DTPA in hyaluronan, gelatin, and composite materials are presented in Table 4.

The Gd-DTPA R1 and R2 values increased between 18–31% and 14–32%, respectively, with increasing concentration of hyaluronan, gelatin, and composite (Table 4; Fig. 2). Statistical significance was achieved in R1 of Gd-DTPA in 50 g/l and 100 g/l hyaluronan compared to Magnevist (Gd-DTPA) in PBS (p=0.038 and p<0.001, respectively). The R1 value of Gd-DTPA was also significantly different (p< 0.001) in the 100 g/l composite compared to Gd-DTPA in PBS. R2 values of Gd-DTPA in hyaluronan and composite materials were not significantly dependent on concentration, except for the 100 g/l concentrations with p=0.021 and p=0.002, respectively.

These data are from different stock solutions than the data presented in Tables 2 and 3, and thus small differences in relaxivity between the experimental periods were found.

Discussion

Hydrogels formed from hydroxyphenyl-substituted hyaluronan [33, 35–42] and gelatin [42–45] are currently being applied to a variety of tissue engineering and repair applications including cartilage [33] and tendon [41] repair, treatment of mitral regurgitation [37, 40] and rheumatoid arthritis [42], and as a dermal filler [35]. In addition, these biomaterials are being investigated as protein or drug delivery systems [36, 38, 39, 42, 44], and 3D culture systems for cell encapsulation or attachment [33, 43–45]. Dityramine cross-linked hyaluronan-based hydrogels [33] were selected as a synthetic ECM model because of the equivalence of their biochemical and mechanical properties compared to cartilage. In addition, the hydrogels can be easily manipulated in terms of concentration and composition, unlike biologic tissues. It is important to characterize the imaging properties of this ECM model because of the breadth of clinical applications being investigated. While the gelatin used in this study is a type-I collagen, previous publications have indicated dGEMRIC results are independent of collagen type [1–3, 6]. Thus, the hydrogels are ideal materials from which to make models of tissue ECM.

Composite ECM hydrogels at concentrations of GAG and collagen similar to those found in native cartilage (50–100 g/l) produced T1 values characteristic of cartilage (700–1,250 ms) [5, 32, 50], although T2 values were much longer than for cartilage and therefore the hydrogels could be easily differentiated from cartilage on any MR acquisition. The non-enhanced material T1 and T2 relaxation times were found to depend very little on extracellular matrix hyaluronan (i.e., GAG) and collagen concentration. This small dependence was reproducible and the combination of hyaluronan and collagen in composite materials yield a synergistic effect on T1 and T2 compared to each material alone.

With increasing concentrations of hyaluronan, gelatin, and/or agar, a decrease in R1 and R2 values was measured, which corresponds to a decrease in water mobility and formation of a more solid-like material. Tyramine-substitution was found to have a slight, but non-significant effect on the relaxivity of either hyaluronan or gelatin alone and the 1:1 composite. This is in agreement with the tyramine-substituted solutions forming solids or semi-solids similar to their corresponding unsubstituted solutions, and having immeasurably small impact on water mobility. Cross-linking had a small statistically significant impact on the R2 values for TB-hyaluronan compared to hyaluronan and TS-HA, and the R2 values for TB-CO compared to composite and TS-CO.

In the past few years, dGEMRIC clinical research studies have measured the GAG concentration of articular cartilage in the knee [1–4, 6, 9, 10, 14–16, 19, 20, 24, 25, 28, 30, 31], hip [18, 21, 22, 25, 26], cartilage repair [20, 28], and also in the fibrocartilaginous meniscus in the knee [11, 17]. Most studies calculated GAG concentration from fixed charge density (FCD) using pre- and post-contrast T1 values. More recently, studies correlate only the post-contrast T1 values with GAG concentration since the pre-contrast T1 value of healthy, normal cartilage has been found to be constant [20, 30]. Using either approach, assuming Gd-DTPA relaxivity in tissues is invariant and identical to that in saline may result in calculation of incorrect FCD and thus incorrect GAG concentration.

The dependence of the Gd-DTPA R1 in cartilage has been previously investigated [6, 8, 9] with conflicting results. One manuscript reports the Gd-DTPA R1 in cartilage as independent of GAG concentration [6]. Another study concluded that macromolecular concentration (but not molecule type) can increase the R1 of Gd-DTPA in cartilage by values 30–70% higher than in saline [8]. Gillis et al. [9] measured the R1 of Gd-DTPA in trypsin digested cartilage plugs and found the relaxivity was influenced by the level of GAG depletion. At 2 T, the range of post-Gd-DTPA cartilage T1 values was found to be 300 ms with a 1.4 mM^{-1} s^{-1} range of R1 values between intact and trypsinized cartilage [9]. In spite of this result, the authors advocate ignoring the compositional dependence of relaxivity because of the operational difficulty in measurement, even though this assumption leads to an underestimation of Gd-DPTA concentration and hence an overestimation of GAG. While it is difficult to manipulate the individual components of in vivo or ex vivo cartilage in a controlled and uniform manner, it is possible using a synthetic extracellular matrix (TB-CO) model system as presented here.

At the higher macromolecular concentrations, our 3 T measurements (Table 4) found statistically different relaxivity values as a function of macromolecular concentration and supports the findings of Stanisz et al. [8] and Gillis et al. [9]. At the lower macromolecular concentrations, our statistically similar 3 T relaxivity values support the findings of Bashir et al. [6]. However, collagen (i.e. gelatin) had twice the impact than hyaluronan on both the R1 and R2 of Gd-DTPA (Table 4, *p*Fig. 2). The relaxivity of Gd-DTPA increased up to 18–31% for R1 and up to 14–32% for R2 with increasing macromolecular concentration. Statistically significant differences in R1 were found for Gd-DTPA in hyaluronan at 50 g/l (=0.038) and 100 g/l ($p<0.001$), composite at 100 g/l ($p<0.001$), and for R2 of Gd-DTPA in hyaluronan and composite at 100 g/l ($p=0.021$ and $p=0.002$, respectively). Thus the R1 of Gd-DTPA in hyaluronan and composite are only comparable to the relaxivity in saline when the macromolecular concentration is below 50 g/l. Since 100 g/l hyaluronan or GAG concentration is similar to that in healthy cartilage [1], the R1 of Gd-DTPA in cartilage can be treated as a constant and identical to that in saline only when the GAG concentration is less than 50% of its value in healthy cartilage.

If the true R1 value is lower than that used in calculations, the tissue Gd-DTPA concentration would be falsely underestimated and interpreted as a higher cartilage (or

meniscal) fixed charge density (FCD), meaning greater tissue repulsion of the negative contrast agent, which results from higher GAG concentrations. For example, if a dGEMRIC map indicated a 75% GAG loss based on a constant R1 of Gd-DTPA, it would actually represent a 90% GAG loss once the compositional dependence of R1 was included in the calculation [9], thereby causing modestly GAG-depleted cartilage to be incorrectly classified as more “normal” or less impacted tissue. Conversely, a 20–30% decrease in the true Gd-DTPA R1 value would result in a 16–24% underestimation of tissue Gd-DTPA concentration and a 5–15% overestimation of tissue GAG and FCD concentration. In addition, the cartilage T1 value at which charge balance occurs (based on an R1 value of 4.64/mM/s) would decrease at 3 T from 485 ms to 465 ms. This threshold is useful for identification of 50% GAG-depletion, and while the 20 ms decrease is within measurement variability it maybe significant as patient disease classification may change. In addition, similar-sized changes have previously resulted in significant ($p<0.05$) group mean differences [16, 19, 23, 29].

Conclusions

This study has laid the groundwork to monitor changes in concentration induced by loss of material following implantation of the TB-hydrogels, using T1 and T2 relaxation time measurements. Using the synthetic extracellular matrix system composed of hyaluronan (GAG) and collagen, we confirmed the relaxivity dependence on tissue macromolecule concentration and type. The variable cartilage Gd-DTPA R1 values are unlikely to change the significance of group mean or pre- versus post-contrast T1 differences. Hence, there is little potential impact on most clinical research studies. However, the variations due to cartilage compositions will slightly change interpretation of clinical results by expanding the range post-contrast T1 values for “normal” tissue. If FCD or GAG concentration values are important to an investigation (for example, in cartilage repair), tissue-specific Gd-DPTA relaxivity incorporated into an iterative FCD calculation may improve results [12, 20, 27]. To incorporate the dGEMRIC technique into clinical practice, it is necessary to compare post-contrast cartilage T1 values to standardized ranges of values for different degrees of cartilage GAG depletion. Proper attention to the compositional variability of cartilage R1 values, when creating standardized cartilage dGEMRIC index values, may help improve the accuracy of dGEMRIC for estimation of osteoarthritis disease severity.

Acknowledgments

The authors would like to thank Amit Vasanji, PhD for help with the image analysis. EL would like to thank the Cleveland State University Doctoral Dissertation Research Expense Award and Lifecore Biomedical, Inc. for their financial support during her PhD and dissertation work. Neither had any involvement in the study design, collection, analysis and interpretation of data, the writing of the manuscript, or the decision to submit the manuscript for publication.

Funding sources EL received a Cleveland State University Doctoral Dissertation Research Expense Award and support from Lifecore Biomedical, Inc. during her dissertation research period. Creation of the gelatin portion of this work was partially funded by a grant from the National Institutes of Health (1-R21-DK077668-01).

References

1. Burstein D, Gray M, Mosher T, Dardzinski B. Measures of molecular composition and structure in osteoarthritis. Radiol Clin N Am. 2009; 47:675–86. [PubMed: 19631075]
2. Blumenkrantz G, Majumdar S. Quantitative magnetic resonance imaging of articular cartilage in osteoarthritis. Eur Cell Mater. 2007; 13:76–86. [PubMed: 17506024]
3. Taylor C, Carballido-Gamio J, Majumdar S, Li X. Comparison of quantitative imaging of cartilage for osteoarthritis: T2, T1ρ, dGEMRIC and contrast-enhanced computed tomography. Magn Reson Imaging. 2009; 27:779–84. [PubMed: 19269769]

4. Gray ML, Eckstein F, Peterfy C, Dahlberg L, Kim YJ, Sorensen AG. Toward imaging biomarkers for osteoarthritis. Clin Orthop Relat Res. 2004; 427:S175–81. [PubMed: 15480063]
5. Stanisz GJ, Odrobina EE, Pun J, Escaravage M, Graham SJ, Bronskill MJ, et al. T1, T2 relaxation and magnetization transfer in tissue at 3 T. Magn Reson Med. 2005; 54:507–12. [PubMed: 16086319]
6. Bashir A, Gray ML, Hartke J, Burstein D. Nondestructive imaging of human cartilage glycosaminoglycan concentration by MRI. Magn Reson Med. 1999; 41:857–65. [PubMed: 10332865]
7. Donahue KM, Burstein D, Manning WJ, Gray ML. Studies of Gd-DTPA relaxivity and proton exchange rates in tissue. Magn Reson Med. 1994; 32:66–76. [PubMed: 8084239]
8. Stanisz GJ, Henkelman RM. Gd-DTPA relaxivity depends on macromolecular content. Magn Reson Med. 2000; 44:665–7. [PubMed: 11064398]
9. Gillis A, Gray M, Burstein D. Relaxivity and diffusion of gadolinium agents in cartilage. Magn Reson Med. 2002; 48:1068–71. [PubMed: 12465119]
10. Wei L, Scheidegger R, Wu Y, Edelman RR, Farley M, Krishnan N, et al. Delayed contrast-enhanced MRI of cartilage: comparison of nonionic and ionic contrast agents. Magn Reson Med. 2010; 64:1267–73. [PubMed: 20648681]
11. Wei L, Edelman RR, Prasad PV. Delayed contrast enhanced MRI of meniscus with ionic and non-ionic agents. J Magn Reson Imaging. 2011; 33:731–5. [PubMed: 21563259]
12. Watanabe A, Boesch C, Anderson SE, Brehm W, Mainil Varlet P. Ability of dGEMRIC and T2 mapping to evaluate cartilage repair after microfracture: a goat study. Osteoarthr Cartil. 2009; 17:1341–9. [PubMed: 19410029]
13. Majumdar S, Sostman HD, MacFall JR. Contrast and accuracy of relaxation time measurements in acquired and synthesized multi-slice magnetic resonance images. Investig Radiol. 1989; 24 (2): 119–27. [PubMed: 2917832]
14. Eckstein E, Mosher T, Hunter DJ. Imaging of knee osteoarthritis: data beyond the beauty. Curr Opin Rheumatol. 2007; 19:435–43. [PubMed: 17762608]
15. Eckstein F, Le Graverand MP, Charles HC, Hunter DJ, Kraus VB, Sunyer T, et al. Clinical, radiographic, molecular and MRI-based predictors of cartilage loss in knee osteoarthritis. Ann Rheum Dis. 2011; 70:1223–30. [PubMed: 21622772]
16. Neuman P, Tjornstrand J, Svensson J, Ragnarsson C, Roos H, Englund M, et al. Longitudinal assessment of femoral knee cartilage quality using contrast enhanced MRI (dGEMRIC) in patients with anterior cruciate ligament injury – comparison with asymptomatic volunteers. Osteoarthr Cartil. 2011; 19(8):977–83. [PubMed: 21621622]
17. Mayerhoefer ME, Mamisch TC, Riegler G, Welsch GH, Dobrocky T, Weber M, et al. Gadolinium diethylenetriaminepentaacetate enhancement kinetics in the menisci of asymptomatic subjects: a first step towards a dedicated dGEMRIC (delayed gadolinium-enhanced MRI of cartilage)-like protocol for biochemical imaging of the menisci. NMR Biomed. epub 2011 Mar24.
18. Mamisch TC, Kain MS, Bittersohl B, Apprich S, Werlen S, Beck M, et al. Delayed gadolinium-enhanced magnetic resonance imaging of cartilage (dGEMRIC) in femoroacetabular impingement. J Orthop Res. 2011; 29(9):1305–11. [PubMed: 21437964]
19. McAlindon TE, Nuite M, Krishnan N, Ruthazer R, Price LL, Burstein D, et al. Change in knee osteoarthritis cartilage detected by delayed gadolinium enhanced magnetic resonance imaging following treatment with collage hydrolysate: a pilot randomized controlled trial. Osteoarthr Cartil. 2011; 19:399–405. [PubMed: 21251991]
20. Trattnig S, Winalski CS, Marlovits S, Jurvelin JS, Welsch GH, Potter HG. Magnetic resonance imaging of cartilage repair: a review. Cartilage. 2011; 2:5–26.
21. Bittersohl B, Hosalkar HS, Kim YJ, Werlen S, Siebenrock KA, Mamisch TC. Delayed gadolinium-enhanced magnetic resonance imaging (dGEMRIC) of hip joint cartilage in femoroacetabular impingement (FAI): are pre- and post-contrast imaging both necessary? Magn Reson Med. 2009; 62:1362–7. [PubMed: 19859935]
22. Pollard TC, McNally EG, Wilson DC, Wilson DR, Madler B, Watson M, et al. Localized cartilage assessment with three-dimensional dGEMRIC in asymptomatic hips with normal morphology and cam deformity. J Bone Joint Surg Am. 2010; 92:2557–69. [PubMed: 21048174]

23. Van Ginckel A, Baelde N, Almqvist KF, Roosen P, McNair P, Witvrouw E. Functional adaptation of knee cartilage in asymptomatic female novice runners compared to sedentary controls. Osteoarthr Cartil. 2010; 18:1564–9. [PubMed: 20950697]
24. Tiderius CJ, Sandin J, Svensson J, Dahlberg LE, Jacobsson L. Knee cartilage quality assessed with dGEMRIC in rheumatoid arthritis patients before and after treatment with a TNF inhibitor. Acta Radiol. 2010; 51:1034–7. [PubMed: 20942734]
25. Bittersohl B, Hosalkar HS, Apprich S, Werlen SA, Siebenrock KA, Mamisch TC. Comparison of pre-operative dGEMRIC imaging with intra-operative findings in femoroacetabular impingement: preliminary findings. Skelet Radiol. 2011; 40:553–61.
26. Fleming BC, Oksendahl HL, Mehan WA, Portnoy R, Fadale PD, Hulstyn MJ, et al. Delayed Gadolinium-enhanced MR Imaging of Cartilage (dGEMRIC) following ACL injury. Osteoarthr Cartil. 2010; 18:662–7. [PubMed: 20188685]
27. Vasiliadis HS, Danielson B, Ljungberg M, McKeon B, Lindahl A, Peterson L. Autologous chondrocyte implantation in cartilage lesions of the knee: long-term evaluation with magnetic resonance imaging and delayed gadolinium-enhanced magnetic resonance imaging technique. Am J Sports Med. 2010; 38:943–9. [PubMed: 20185841]
28. Zilkens C, Holstein A, Bittersohl B, Jaeger M, Haamberg T, Miese F, et al. Delayed gadolinium-enhanced magnetic resonance imaging of cartilage in the long-term follow-up after Perthes disease. J Pediatr Orthop. 2010; 30:147–53. [PubMed: 20179562]
29. Yao W, Qu N, Lu Z, Yang S. The application of T1 and T2 relaxation time and magnetization transfer ratios to the early diagnosis of patellar cartilage osteoarthritis. Skelet Radiol. 2009; 38:1055–62.
30. Li W, Du H, Scheidegger R, Wu Y, Prasad PV. Value of precontrast T1 for dGEMRIC of native articular cartilage. J Magn Reson Imaging. 2009; 29:494–7. [PubMed: 19161210]
31. Sasaki M, Shibata E, Kanbara Y, Ehara S. Enhancement effects and relaxivities of gadolinium-DTPA at 1.5 versus 3 Tesla: a phantom study. Magn Reson Med Sci. 2005; 4:145–9. [PubMed: 16462135]
32. Williams A, Mikulis B, Krishnan N, Gray M, McKenzie C, Burstein D. Suitability of T1Gd as the “dGEMRIC Index” at 1.5 T and 3.0 T. Magn Reson Med. 2007; 58:830–4. [PubMed: 17899599]
33. Darr A, Calabro A. Synthesis and characterization of tyramine-based hyaluronan hydrogels. J Mater Sci Mater Med. 2009; 20:33–44. [PubMed: 18668211]
34. Gross AJ, Sizer IW. The oxidation of tyramine, tyrosine, and related compounds by peroxidase. J Biol Chem. 1959; 234:1611–4. [PubMed: 13654426]
35. Chan J, Darr AB, Alam D, Calabro A. Investigation of a novel cross-linked hyaluronan hydrogel for use as a soft-tissue filler. Am J Cosmetic Sur. 2005; 22:105–8.
36. Kurisawa M, Chung JE, Yang YY, Gao SJ, Uyama H. Injectable biodegradable hydrogels composed of hyaluronic acid-tyramine conjugates for drug delivery and tissue engineering. Chem Commun (Camb). 2005; 34:4312–4. [PubMed: 16113732]
37. Kamohara K, Banbury M, Calabro A, Popovic ZB, Darr A, Ootaki Y, et al. A novel technique for functional mitral regurgitation therapy: mitral annular remodeling. Heart Surg Forum. 2006; 9:E888–92. [PubMed: 17599888]
38. Lee F, Chung JE, Kurisawa M. An injectable enzymatically cross-linked hyaluronic acid-tyramine hydrogel system with independent tuning of mechanical strength and gelation rate. Soft Matter. 2008; 4:880–7.
39. Lee F, Chung JE, Kurisawa M. An injectable hyaluronic acid-tyramine hydrogel system for protein delivery. J Control Release. 2009; 134:186–93. [PubMed: 19121348]
40. Fumoto H, Takaseya T, Shiose A, Saraiva RM, Arakawa Y, Park M, et al. Mitral annular remodeling to treat functional mitral regurgitation: a pilot acute study in a canine model. Heart Surg Forum. 2010; 13:E247–50. [PubMed: 20719728]
41. Chin LK, Calabro A, Rodriguez ER, Tan CD, Walker E, Derwin KA. Characterization of and host response to tyramine substituted-hyaluronan enriched fascia extracellular matrix. J Mater Sci Mater Med. 2011; 22(6):1465–77. [PubMed: 21553156]

42. Kim KS, Park SJ, Yang J-A, Jeon J-H, Bhang SH, Kim B-S, et al. Injectable hyaluronic acid-tyramine hydrogels for the treatment of rheumatoid arthritis. Acta Biomater. 2011; 7:666–74. [PubMed: 20883838]

43. Hu M, Kurisawa M, Deng R, Teo CM, Schumacher A, Thong YX, et al. Cell immobilization in gelatin-hydroyphenylproprionic acid hydrogel fibers. Biomaterials. 2009; 30:3523–31. [PubMed: 19328545]

44. Sakai S, Hirose K, Taguchi K, Ogushi Y, Kawakami K. An injectable, in situ enzymatically gellable, gelatin derivative for drug delivery and tissue engineering. Biomaterials. 2009; 30:3371–7. [PubMed: 19345991]

45. Wang LS, Chung JE, Chan PP, Kurisawa M. Injectable biodegradable hydrogels with tunable mechanical properties for the stimulation of neurogenesic differentiation of human mesenchymal stem cells in 3D culture. Biomaterials. 2010; 31:1148–57. [PubMed: 19892395]

46. Lou X, Chirila TV. Swelling behavior and mechanical properties of chemically cross-linked gelatin for biomedical use. J Biomater Appl. 1999; 14:185–91.

47. Spackman DH, Stein WH, Moore S. Automatic recording apparatus for use in the chromatography of amino acids. Anal Chem. 1958; 30:1190–206.

48. Blumenkrantz N, Asboe-Hansen G. New method for quantitative determination of uronic acid. Anal Biochem. 1973; 54:484–9. [PubMed: 4269305]

49. Mulkern RV, Wong ST, Jakab P, Bleier AR, Sandor T, Jolesz FA. CPMG imaging sequences for high field in vivo transverse relaxation studies. Magn Reson Med. 1990; 16:67–79. [PubMed: 2255238]

50. Gold G, Han E, Stainsby J, Wright G, Brittain J, Beaulieu C. Musculoskeletal MRI at 3.0 T: relaxation times and image contrast. Am J Roentgenol. 2004; 183:343–51. [PubMed: 15269023]

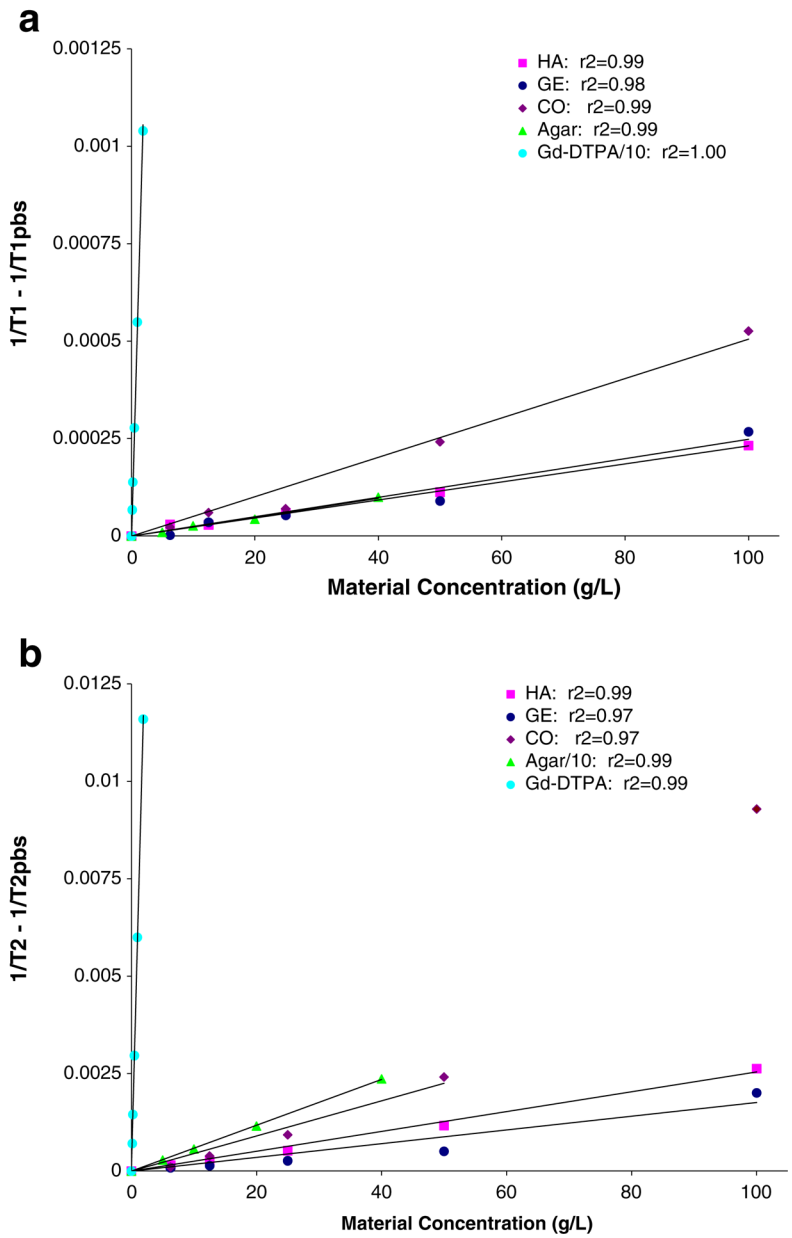

Fig. 1.

a Material spin–lattice relaxivity (R1). R1 is the slope of the plot [$1/T1 - 1/T1_{pbs}$] versus material concentration (g/l) for unsubstituted hyaluronan (HA), gelatin (GE) and HA/GE composite (CO) materials as well as Gd-DTPA (Gd) and agar controls from a single imaging session. The Gd-DTPA values were divided by ten to enable them to be plotted on the same scale as agar and the hydrogels. **b** Material spin-spin relaxivity (R2). R2 is the slope of the plot of [$1/T2 - 1/T2_{pbs}$] versus material concentration (g/l) for unsubstituted HA, GE and CO materials as well as Gd and agar controls from a single imaging session. The agar values were divided by ten to enable them to be plotted on the same scale as Gd-DTPA and the hydrogels

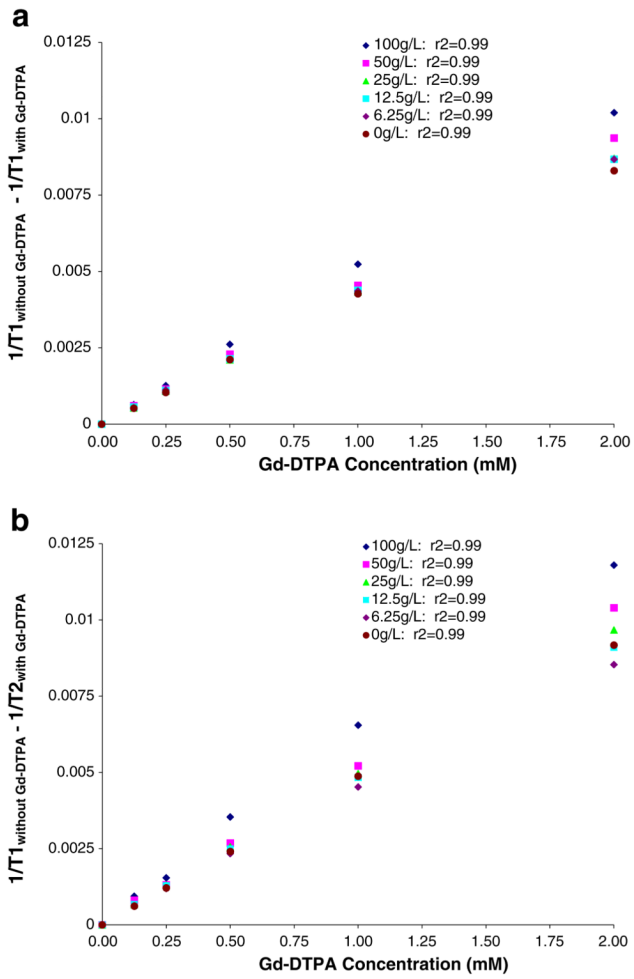

Fig. 2.

a Effect of macromolecular concentration on Gd-DTPA spin–lattice relaxivity (R1). Plot of unsubstituted hyaluronan/collagen composite (CO) material concentration (g/l) versus the R1 of Gd-DTPA (mM) from a single imaging session. The slope of the R1 curves linearly increased with increasing concentration of CO. **b** Effect of macromolecular concentration on Gd-DTPA spin-spin relaxivity (R2). Plot of unsubstituted CO material concentration (g/l) versus the R2 of Gd-DTPA (mM) from a single imaging session. The slope of the R2 curves linearly increased with increasing concentration of CO

Table 1

Material compositions and abbreviations. All samples were prepared in PBS except TB-GE, which were prepared in ultra-pure water

Sample	Description	Concentrations
HA	Hyaluronan	6.25, 12.5, 25, 50, 100 (g/l)
GE	Gelatin	6.25, 12.5, 25, 50, 100 (g/l)
CO	Composite (1:1 HA:GE)	6.25, 12.5, 25, 50, 100 (g/l)
TS-HA	Tyramine-substituted HA	6.25, 12.5, 25, 50, 100 (g/l)
TS-GE	Tyramine-substituted GE	6.25, 12.5, 25, 50, 100 (g/l)
TS-CO	Tyramine-substituted CO	6.25, 12.5, 25, 50, 100 (g/l)
TB-HA	Tyramine-based HA (cross-linked)	6.25, 12.5, 25, 50, 100 (g/l)
TB-GE	Tyramine-based GE (cross-linked)	6.25, 12.5, 25, 50, 100 (g/l)
TB-CO	Tyramine-based CO (cross-linked)	6.25, 12.5, 25, 50, 100 (g/l)
Agar	Agar	0.5, 1, 2, 4 (weight %)
Gd	Magnevist ($Gd\text{-}DTPA^{-2}$)	0.125, 0.25, 0.5, 1, 2 (mM)

Table 2

T1 and T2 values from single imaging sessions. Equivalent concentrations of agar were 0.5, 1, 2, and 4 wt%. Equivalent concentrations of Gd-DTPA were 0.125, 0.25, 0.5, 1, and 2 mM. PBS was used for 0 concentration samples for all compositions except TB-GE where ultra-pure water was used. *HA* hyaluronan; *GE* gelatin; *CO* composite, 1:1 HA:GE; *TS-HA* tyramine-substituted HA; *TS-GE* tyramine-substituted GE; *TS-CO* tyramine-substituted CO; *TB-HA* tyramine-based HA - Cross-linked); *TB-GE* tyramine-based GE -Cross-linked); *TB-CO* tyramine-based CO - cross-linked; Agar; *Gd* Magnevist, Gd-DTPA^{-2}

Unsubstituted Materials			**Tyramine-substituted Materials**			**Cross-linked Materials**		
HA (g/l)	**T1 (ms)**	**T2 (ms)**	**TS-HA (g/l)**	**T1 (ms)**	**T2 (ms)**	**TB-HA (g/l)**	**T1 (ms)**	**T2 (ms)**
0	2,469±179	1,325±48	0	2,469±179	1,325±48	0	2,730±188	1,380±62
6.25	2,219±112	1,144±26	6.25	2,388±209	1,110±31	6.25	2,509±170	1,096±38
12.5	2,183±132	1,008±22	12.5	2,228±124	988±18	12.5	2,284±196	917±190
25	2,051±158	821±13	25	2,108±104	808±16	25	2,223±114	745±87
50	1,835±133	536±7	50	1,809±65	551±7	50	1,891±131	513±35
100	1,482±48	309±5	100	1,461±56	282±11	100	1,390±111	264±257
GE (g/l)	T1 (ms)	T2 (ms)	TS-GE (g/l)	T1 (ms)	T2 (ms)	TB-GE (g/l)	T1 (ms)	T2 (ms)
0	2,469±179	1,325±48	0	2,469±179	1,325±48	0	2,716±198	1,556±103
6.25	2,332±126	1,169±33	6.25	2,244±124	1,134±32	6.25	2,479±155	1,176±40
12.5	2,305±195	1,075±27	12.5	2,226±132	1,039±20	12.5	2,344±180	1,259±28
25	2,177±218	976±17	25	2,067±125	886±10	25	2,133±132	1,038±44
50	1,751±84	607±24	50	1,913±59	679±13	50	1,765±112	711±168
100	1,122±49	264±9	100	1,590±56	409±9	100	1,529±237	475±61
CO (g/l)	T1 (ms)	T2 (ms)	TS-CO (g/l)	T1 (ms)	T2 (ms)	TB-CO (g/l)	T1 (ms)	T2 (ms)
0	2,469±179	1,325±48	0	2,469±179	1,325±48	0	2,730±188	1,380±62
6.25	2,311±204	1,079±20	6.25	2,327±118	1,000±17	6.25	2,485±106	991±100
12.5	2,257±107	855±67	12.5	2,115±88	790±19	12.5	2,065±276	745±126
25	2,137±138	474±6	25	1,829±96	568±32	25	1,627±158	417±99
50	1,371±135	287±31	50	1,266±34	237±4	50	1,360±126	376±62
100	760±279	77±10	100	809±27	95±3	100	978±38	139±62
Agar (g/l)	T1 (ms)	T2 (ms)						
0	2,469±179	1,325±48						
5	2,173±177	288±5						
10	2,033±105	162±3						

Unsubstituted Materials			Tyramine-substituted Materials			Cross-linked Materials		
HA (g/l)	T1 (ms)	T2 (ms)	TS-HA (g/l)	T1 (ms)	T2 (ms)	TB-HA (g/l)	T1 (ms)	T2 (ms)
20	1,942±191	85±2						
40	1,646±78	44±3						
Gd (g/l)	T1 (ms)	T2 (ms)						
0	2,469±179	1,325±48						
0.12	1,036±30	661±15						
0.23	634±13	441±8						
0.47	352±7	260±4						
0.94	189±4	142±3						
1.88	98±3	76±3						

Table 3

Average relaxivity (R1 and R2) values. *N* is the number of imaging sessions. The hydrogels and MR instrumentation showed stability over time as indicated by the small standard deviation obtained from measurements performed repeatedly over several months. R2 values for HA (p=0.007) and TS-HA (p=0.012) were significantly different than for TB-HA (cross-linked). R2 values for CO (p=0.020) and TS-CO (p=0.019) were significantly different than for TB-CO (cross-linked). *HA* hyaluronan; *GE* gelatin; *CO* composite, 1:1 HA:GE; *TS-HA* tyramine-substituted HA; *TS-GE* tyramine-substituted GE); *TS-CO* (tyramine-substituted CO); *TB-HA* (tyramine-based HA - cross-linked); *TB-GE* tyramine-based GE - cross-linked; *TB-CO* tyramine-based CO -cross-linked; Agar; *Gd* Magnevist, Gd-DTPA^{-2}

Sample	R1 (l g^{-1} s^{-1})	R2 (l g^{-1} s^{-1})	N
HA	0.0027±0.0003	0.025±0.003	5
TS-HA	0.0030±0.0004	0.027±0.003	4
TB-HA	0.0033±0.0003	0.036±0.006	4
GE	0.0032±0.0010	0.020±0.006	5
TS-GE	0.0021±0.0004	0.016±0.001	4
TB-GE	0.0029±0.0006	0.015±0.002	4
CO	0.0068±0.0018	0.101±0.014	4
TS-CO	0.0085±0.0000	0.099±0.000	2
TB-CO	0.0062±0.0001	0.062±0.001	2
1 Agar	0.0028±0.0011	0.59±0.05	5
2 Gd	5.65±0.34	6.4±0.39	5

1 Agar relaxivity units: wt %$^{-1}$ s^{-1}

2 Gd relaxivity units: mM^{-1} s^{-1}

Table 4

Average R1 and R2 values of Gd-DTPA (Gd) with different concentrations of macromolecular materials. *N* is the number of imaging sessions. The hydrogels and MR instrumentation showed stability over time as indicated by the small standard deviation obtained from measurements performed repeatedly over several months. Relaxivities are compared to Gd-DTPA in PBS with statistically significant differences achieved in HA at concentrations above 50 g/l and in CO at 100 g/l. The R1 of Gd-DTPA in 100 g/l HA, GE and CO is 18, 31, and 20%, respectively, larger than in PBS. *HA* hyaluronan; *GE* gelatin; *CO* composite, 1:1 HA:GE

Sample	(g/l)	R1 (mM^{-1} s^{-1})	N	p-value (R1)	R2 (mM^{-1} s^{-1})	N	p-value (R2)
HA	6.25	4.34±0.08	3	0.471	4.88±0.16	3	0.470
	12.5	4.31±0.10	3	0.421	4.92±0.16	3	0.615
	25	4.41±0.12	3	0.204	4.96±0.19	3	0.625
	50	4.51±0.10	3	0.038	5.09±0.21	3	0.341
	100	4.99±0.11	3	<0.001	5.43±0.34	3	0.021
GE	6.25	4.22	1		4.71	1	
	12.5	4.34	1		4.80	1	
	25	4.45	1		4.99	1	
	50	4.90	1		5.34	1	
	100	5.55	1		6.27	1	
CO	6.25	4.28±0.12	3	0.783	4.60±0.44	3	0.810
	12.5	4.29±0.08	3	0.933	4.81±0.32	3	0.659
	25	4.38±0.10	3	0.773	5.03±0.28	3	0.459
	50	4.64±0.16	3	0.103	5.46±0.33	3	0.059
	100	5.10±0.35	3	<0.001	6.11±0.36	3	0.002
PBS		4.24±0.08	3		4.75±0.18	3	